Published in final edited form as:
J Membr Biol. 2009 March ; 228(1): 1–14. doi:10.1007/s00232-009-9154-8.

Regulation of the Kv2.1 potassium channel by MinK and MiRP1

Zoe A. McCrossan[†], **Torsten K. Roepke**[†], **Anthony Lewis**, **Gianina Panaghie**, and **Geoffrey W. Abbott**[*]
Greenberg Division of Cardiology, Departments of Medicine and Pharmacology, Weill Medical College of Cornell University, New York, NY

Abstract

Kv2.1 is a voltage-gated potassium (Kv) channel α subunit expressed in mammalian heart and brain. MinK-related peptides (MiRPs), encoded by *KCNE* genes, are single transmembrane domain ancillary subunits that form complexes with Kv channel α subunits to modify their function. Mutations in human MinK (KCNE1) and MiRP1 (KCNE2) are associated with inherited and acquired forms of long QT syndrome (LQTS). Here, co-immunoprecipitations from rat heart tissue suggested that both MinK and MiRP1 form native cardiac complexes with Kv2.1. In whole-cell voltage clamp studies of subunits expressed in CHO cells, rat MinK and MiRP1 reduced Kv2.1 current density 3- and 2-fold respectively, slowed Kv2.1 activation (at +60 mV) 2- and 3-fold respectively, and each slowed Kv2.1 deactivation <2-fold. Human MinK slowed Kv2.1 activation 25%, while human MiRP1 slowed Kv2.1 activation and deactivation 2-fold. Inherited mutations in human MinK and MiRP1, previously associated with LQTS, were also evaluated. D76N-MinK and S74L-MinK reduced Kv2.1 current density (3-fold and 40%, respectively) and slowed deactivation (60 and 80%, respectively). Compared to wild-type human MiRP1-Kv2.1 complexes, channels formed with M54T- or I57T-MiRP1 showed greatly slowed activation (10-fold and 5-fold, respectively). The data broaden the potential roles of MinK and MiRP1 in cardiac physiology and support the possibility that inherited mutations in either subunit could contribute to cardiac arrhythmia by multiple mechanisms.

Keywords

potassium channel; long QT syndrome; KCNE1; KCNE2

INTRODUCTION

Voltage-gated potassium (Kv) channel pore-forming α subunits open in response to cellular depolarization to allow outward K^+ ion diffusion, mediating cellular repolarization. *KCNE* genes encode single transmembrane domain ancillary peptides termed MinK-Related Peptides, or MiRPs. MiRPs form complexes with Kv channel α subunits to modulate their function, helping generate the broad array of Kv currents observed in excitable cells. MinK (*KCNE1*) and MiRPs 1 through 4 (*KCNE2-5*) transcripts have all been detected in human heart (Abbott et al., 1999; Chen et al., 2003; Piccini et al., 1999). MinK associates with the KCNQ1 Kv channel α subunit to form the I_{Ks} ventricular repolarization current in human heart; MiRP1 modulates the hERG α subunit which forms the cardiac I_{Kr} repolarization current in human heart. Inherited mutations in human MinK, MiRP1, KCNQ1 and hERG account for four variants of inherited long QT syndrome (LQTS), and MiRP1 mutations are also associated

*To whom correspondence should be addressed: Starr 463, Greenberg Division of Cardiology, Weill Medical College of Cornell University, 1300 York Avenue, New York, NY, 10065. Tel: 212 746 6275; Fax: 212 746 7984 gwa2001@med.cornell.edu.
[†]These authors contributed equally

with acquired LQTS (Sesti et al., 2000). The known partnering promiscuity of MiRPs in heterologous expression experiments raises the possibility that MinK and MiRP1 might perform multiple roles in the heart and other tissues.

Kv2.1 is a delayed rectifier potassium channel ubiquitously expressed in the brain, where it controls excitability in a wide range of mammalian neurons (Antonucci et al., 2001; Du et al., 1998; Frech et al., 1989; Murakoshi & Trimmer, 1999). Kv2.1 is also widely expressed in rodent heart (Bou-Abboud, Li & Nerbonne, 2000; Dixon & McKinnon, 1994; Xu et al., 1999; Xu et al., 1999) and is reported to contribute to both $I_{K,slow}$ in mouse ventricles and its equivalent current in murine atria ($I_{K,s}$); and I_{ss} in mouse atria (Bou-Abboud et al., 2000; Bou-Abboud & Nerbonne, 1999). Kv2.1 protein has been detected in human atria (Van Wagoner et al., 1997) and Kv2.1 mRNA is present in human ventricle (Kaab et al., 1998), but to date Kv2.1 lacks a known native current correlate in human heart. In the rat heart Kv2.1 expression is higher in the atrial membranes than in the ventricles (Barry et al., 1995) and Kv2.1 expression is downregulated in models of cardiac hypertrophy (Capuano et al., 2002), myocardial infarction (Huang, Qin & El-Sherif, 2001) and hypothyroidism (Le Bouter et al., 2003).

The functional diversity of Kv2.1 current properties is increased by its ability to associate with a variety of accessory subunits. Modulatory subunits for Kv2.1 include electrically silent Kv α subunits such as Kv5.1, Kv6.1(Post, Kirsch & Brown, 1996), Kv8.1 (Salinas et al., 1997), Kv9.1–9.3 (Salinas et al., 1997) and the KChAP ancillary subunit (Kuryshev et al., 2000). While silent Kv α subunits serve to increase functional diversity of current kinetics by assembling with Kv2.1 subunits to form heterotetrameric channels at the cell surface (all subunits lining the pore), KChAP is cytoplasmic and associates at the intracellular amino terminus of Kv2.1 to produce a significant increase in both Kv2.1 channel protein and the number of functional channels at the cell surface (Kuryshev et al., 2000). We previously showed that MiRP2 forms complexes with Kv2.1 in rat brain, and that in CHO cell co-expression studies MiRP2 slows Kv2.1 activation and deactivation, and increases the extent of inactivation (McCrossan et al., 2003). We also recently generated a *kcne2* null mouse to examine the native roles of MiRP1 (KCNE2). We found that in murine ventricles, MiRP1 co-assembles and functionally regulates Kv1.5 and Kv4.2, but not Kv2.1 (Roepke et al., 2008). The findings of these latter two studies led us to examine whether MinK and MiRP1 were capable of forming complexes with Kv2.1 *in vitro* or *in vivo* in other animal models, and what the functional effects might be.

Here, using native co-immunoprecipitations we detected native MinK-Kv2.1 and MiRP1-Kv2.1 complexes in rat heart tissue, and found that rat and human MinK and MiRP1 modify the gating properties of Kv2.1 channels heterologously expressed in CHO cells. Mutations in human MinK and MiRP1 are thought to underlie LQT syndrome *via* effects on complexes formed with either KCNQ1 or hERG α subunits; here we show that mutations in human MinK and MiRP1 previously associated with inherited LQTS also alter the function of channels formed with Kv2.1. This raises the possibility that MinK or MiRP1 mutations may contribute to cardiac dysfunction via impairment of the function of cardiac channel complexes formed with Kv2.1. Further, the formation of MinK-Kv2.1 complexes *in vivo* could explain the recent findings that *kcne1* null mice exhibit atrial fibrillation, and that these mice show increased atrial myocyte I_K compared to wild-type (Temple et al., 2005), a result inconsistent with effects on I_{Ks} because MinK upregulates KCNQ1 current (Barhanin et al., 1996; Sanguinetti et al., 1996; Sesti & Goldstein, 1998).

METHODS

RT-PCR

Kv2.1, MinK, MiRP1 and MiRP2 RNA expression was detected by RT-PCR. For all native tissue studies in this report, adult Sprague-Dawley rats were housed and utilized according to the NIH Guide for the Care and Use of Laboratory Animals and Weill Medical College of Cornell University animal care and use policies, and humanely euthanized by CO_2 inhalation prior to tissue extraction. Hearts were removed, rinsed, then the tissue frozen and disrupted under liquid nitrogen using a RNA-zap treated mortar and pestle. The frozen tissue was homogenized through a *Qiashredder* (Qiagen). Total RNA was extracted from homogenized samples using the *RNeasy* kit (Qiagen), DNase I cleaned using the on-column *RNase-free* kit (Qiagen), and reverse transcribed using the *Superscript II* First-strand synthesis kit (Invitrogen). Primer sequences were (5′ to 3′): rKv2.1, AGGCCGAACTGTGTCTACTC (sense) and GTCCTCTGCACCCTCCTAAC (antisense);(Conforti & Millhorn, 1997) rMinK, CACAACTGTTCTGCCTTTTCTG (sense) and TTCATGACAGTGGCTTCAGTTC (antisense); rMiRP1, AGGGGGAAACATGACCACTT (sense) and GCAGATGGACTCTCGTTCTT (antisense); rMiRP2, CAGATCGCAGAGTCAGTTTCTAGC (sense) and TCGAGATGAGTTCCGGAGACC (antisense) and gave PCR products of 557 bp, 376bp, 403bp and 596bp, respectively. Gene identities were confirmed by sequencing single bands cut from 1% agarose gels.

Western blotting and co-immunoprecipitation

Protocols for preparation of crude heart plasma membranes and immunoprecipitations were adapted from previous protocols (McCrossan et al., 2003; Pitts, 1979). Frozen whole hearts from adult Sprague-Dawley rats were homogenized, resuspended in 5 ml buffer (per 3 hearts) comprising in mM: 0.6 sucrose, 10 MOPS, plus protease inhibitor cocktail (Boehringer), pH 7.4 and centrifuged for 5 min, 500 × *g*. This and all following centrifugation steps were carried out at 4 °C. The supernatant was re-centrifuged for 30 min, 12,000 × *g*, the pellet discarded and the supernatant diluted to 40ml with buffer comprising in mM: 160 NaCl, 20 MOPS, plus protease inhibitors, pH 7.4. 10 ml of 1M sucrose was added and the solution centrifuged for 1 hour at 160,000 × *g*. The resulting pellet was resuspended in buffer comprising in mM: 54 LiCl, 6 KCl, 100 NaCl, 20 MOPS, plus protease inhibitors, pH 7.4, homogenized by passing through progressively smaller gauge syringe needles, then diluted 10:1 with immunoprecipitation (IP) buffer: 150 mM NaCl, 50 mM Tris-HCL (pH 7.4), 20 mM NaF, 10 mM $NaVO_4$, 1 mM phenylmethylsulfonyl fluoride (Fisher Scientific), 1% Nonidet P-40 (Pierce, Rockford, IL), 1% CHAPS (Sigma, St. Louis, MO), 1% Triton X-100 (Fisher Scientific), and 0.5% SDS (Sigma). The mixture was incubated on a rocking platform for 1 hour at 4 °C, debris removed by centrifugation at 20,000 × *g* for 5 min and the supernatant retained. The supernatant was pre-cleared by incubation with Protein A-Sepharose 4B beads (Pierce) for 30 min, the beads being removed by centrifugation.

The pre-cleared supernatant was incubated with antibodies for immunoprecipitation: anti-Kv2.1 (Sigma), anti-ERG (Sigma), anti-A1 adenosine receptor (A1-R) (Santa Cruz Biotechnology, Santa Cruz, CA) or in-house rabbit polyclonal antibodies raised against MinK, MiRP1 or MiRP2, for 2–16 hours at 4 °C. Protein A-Sepharose 4B beads (Pierce) were then added and the mixture incubated for a further 5 hours at 4 °C. The complexed beads were collected by centrifugation, washed in IP buffer for 4 × 20 min, and then purified complexes were eluted by incubating the beads for 20 min at 37 °C in 5 % β-mercaptoethanol, 1 mM EDTA, 1.5 % SDS and 10 % glycerol in 50 mM Tris buffer, pH 6.7. Post-centrifugation, the resulting bead eluates were heated for a further 20 min at 50 °C and then size-fractionated by SDS-PAGE. Following membrane transfer, blots were probed with primary antibodies as indicated and detected with goat anti-rabbit horseradish peroxidase-coupled secondary

antibodies (BioRad) for fluorography. Western blots were also performed directly on crude membrane fractions to detect expression of subunits in rat heart membrane fractions, and also on lysates from non-transfected CHO cells, and CHO cells transfected with expression plasmids for rat MinK, MiRP1 or MiRP2 (see below).

Cell culture, transfection and immunofluorescence analysis

Chinese Hamster Ovary (CHO) cells were cultured as previously described (McCrossan et al., 2003) and co-transfected with expression vectors containing cDNA encoding rat Kv2.1, GFP and wild-type rat or human variants of MinK, MiRP1, or human mutants (hMinK-D76N, hMinK-S74L, hMiRP1-M54T, hMiRP1-I57T). Standard *Superfect* (Qiagen) transfection protocols were used, then cells were plated on glass coverslips and 24 h allowed for gene expression before whole cell recordings, protein biochemistry or immunofluorescence analysis. Immunofluorescence analysis of Kv2.1 and HA-tagged rat MinK and MiRP1 localization was performed as we previously described (McCrossan et al., 2003).

Electrophysiology

Whole-cell patch clamp recordings of CHO cells expressing subunits as described above were performed at 22–25 °C using an IC50 inverted microscope equipped with epifluorescence optics for GFP detection (Olympus), a Multiclamp 700A Amplifier, a Digidata 1300 Analogue/Digital converter and a PC with pClamp9 software (Axon Instruments, Foster City, CA). CHO Cells were bathed in a physiological solution comprising (in mM) 135 NaCl, 5 KCl, 1.2 $MgCl_2$, 5 HEPES, 2.5 $CaCl_2$, 10 D-Glucose (pH 7.4). Borosilicate glass pipettes (Sutter) were of 3–5 MΩ resistance when filled with intracellular solution containing (in mM) 10 NaCl, 117 KCl, 2 $MgCl_2$, 11 HEPES,11 EGTA, 1 $CaCl_2$ (pH 7.2). Cells were stepped from a holding potential of −80 mV to test potentials between −60 and +60 mV in 10 mV increments for 2 s duration, followed by a tail pulse to −40 mV for 1s duration, repeated at 0.1 Hz. Leak and liquid junction potentials (< 4 mV) were not compensated for when generating current-voltage relationships. Conductance-voltage relationships were determined by plotting tail currents *versus* prepulse voltage. Normalized conductance-voltage relationships were fit with a Boltzmann function, $G = G_{max}/[1 + \exp(V–V_{0.5}/k)]$ where $V_{0.5}$ is the half-maximal activation, and k is the slope factor. Tetraethylammonium (TEA) dose responses were fit with a logistic dose response function, $y = [A_1\text{-}A_2/1 + (x_0/x)^p] + A_2$ where x_0 is the half-maximal inhibition, and p is the slope factor. Data were analyzed using pClamp9 software (Axon Instruments) and statistical analysis (One-way ANOVA) was performed using Origin 6.1 (Microcal) software. Error bars on figures indicate standard error of the mean.

RESULTS

Immunoprecipitation of MinK-Kv2.1 and MiRP1-Kv2.1 complexes from rat heart tissue

Kv2.1, MinK, MiRP1 and MiRP2 transcript expression in whole rat heart was detected using RT-PCR (Figure 1A, B). In-house antibodies raised against MinK, MiRP1 and MiRP2 epitopes were shown to detect rat MinK, MiRP1 and MiRP2 respectively, in transfected CHO cells, and did not detect proteins in non-transfected CHO cells (Figure 1C). Kv2.1, ERG, MinK, MiRP1 and MiRP2 proteins were also detected in rat heart membrane fractions using their respective antibodies (Figure 1D). The multiple bands observed here in some cases for MiRPs are consistent with previous reports of several glycosylated or unglycosylated forms of MiRP subunits being detectable in heterologous or native preparations (Abbott et al., 2001; Abbott et al., 1999). Similarly, α subunits each showed two main bands corresponding to monomeric and multimeric forms, and minor bands presumed to be immature (non-glycosylated) forms.

Immunoprecipitations from rat heart membrane fractions were performed with antibodies raised against Kv2.1, A1-R, MinK, MiRP1, or MiRP2. The resultant immunoprecipitates were

size-fractionated and Western blotted to detect co-immunoprecipitated proteins. Kv2.1 protein was immunoprecipitated from rat heart membranes with anti-Kv2.1, anti-MinK and anti-MiRP1 antibodies ($n = 4$) but not with anti-A1-R or anti-MiRP2 antibodies ($n = 2$) (Figure 1E). MinK was co-immunoprecipitated from rat heart membranes with anti-Kv2.1, anti-ERG and anti-MinK antibodies ($n = 2$) (Figure 1F, upper). MiRP1 was co-immunoprecipitated from rat heart membranes with anti-Kv2.1, anti-ERG and anti-MiRP1 antibodies ($n = 2$) (Figure 1F, lower). In summary, the data suggest that MinK and MiRP1, but not MiRP2, form stable complexes with Kv2.1 and with ERG in rat heart membranes.

Rat MinK and MiRP1 alter Kv2.1 gating in CHO cell expression studies

Cloned Kv2.1 was heterologously expressed with rat MinK or MiRP1 in Chinese Hamster Ovary (CHO) cells, and functional effects quantified using whole-cell voltage clamp recording. Untransfected CHO cells showed no significant whole-cell currents, neither did cells transfected with MinK or MiRP1 alone (data not shown). Transfection of CHO cells with Kv2.1 alone gave moderately fast activating and deactivating, slow-inactivating outward currents at depolarized voltages, as previously reported (Frech et al., 1989) (Figure 2A). Co-expression with rat MinK reduced mean Kv2.1 current density ~3-fold ($p < 0.001$ at +20 to +60 mV, n = 14–42) (Figure 2A, B), without altering the conductance-voltage relationship (data not shown). Figure 2C shows normalization of early (300 ms) portions of traces demonstrating activation to peak at 0 mV. Fitting of activation to peak with a single exponential for each voltage gave an approximation of the time constant of activation (τ). Rat MinK produced a ~2-fold slowing of Kv2.1 activation (at +60 mV: $p < 0.05$, n = 14–42) (Figure 2C, D). Figure 2E shows exemplar traces of deactivation of Kv2.1 alone or with rat MinK at −40 mV in CHO cells. Deactivation at −40 mV was fitted with a double exponential function, revealing that rat MinK slowed both components of Kv2.1 deactivation (τ_{slow}, ms: Kv2.1 alone, 119 ± 9; Kv2.1-rMinK, 201 ± 33; τ_{fast}, ms: Kv2.1 alone, 17 ± 1; Kv2.1-rMinK, 23 ± 1; $p < 0.05$) with a small decrease in the relative amplitude of the slow component of Kv2.1 deactivation (Kv2.1 alone, 0.49 ± 0.02; Kv2.1-rMinK, 0.34 ± 0.03; $p < 0.05$) (Figure 2E-G). Rat MiRP1 had qualitatively similar effects on Kv2.1: a 2-fold reduction in mean current density (Figure 2A, B) and a marked slowing of activation, 3-fold at +60 mV ($p < 1\times10^{-7}$, n = 17–19) (Figure 2C, D). Rat MiRP1 also increased the τof the slow component of Kv2.1 deactivation by 50% ($p < 0.001$; n = 17–19) without altering its relative amplitude compared to Kv2.1 alone (Figure 2E-G). The altered gating of Kv2.1 when co-expressed with rat MinK or MiRP1 suggested the formation of heteromeric channel complexes at the plasma membrane in CHO cells. This was supported by immunofluorescence studies which showed co-localization of Kv2.1 with rat MinK and with rat MiRP1 at the cell surface (Supplementary Figure 1).

Human MiRP1 and MinK alter Kv2.1 gating in CHO cell expression studies

We and others previously demonstrated MinK and MiRP1 species-dependent effects (McCrossan & Abbott, 2004), therefore we next examined functional effects of human MinK and MiRP1 on Kv2.1 using whole-cell voltage-clamp of transfected CHO cells. Co-transfection of human MinK or MiRP1 significantly altered neither mean Kv2.1 current density (Kv2.1, 1182 ± 123 A/F, n = 42; Kv2.1-hMinK, 1022 ± 150 A/F, n = 24; Kv2.1-hMiRP1, 846 ± 120 A/F, n =16) (Figure 3A, B) nor the Kv2.1 conductance-voltage relationship (Figure 3C). In contrast, both subunits slowed Kv2.1 activation; hMiRP1 having significant effects at all positive voltages, and hMinK at +60 mV only (Figure 3D, E). Thus, the τof Kv2.1 activation at +60 mV was doubled by human MiRP1 and increased 25% by human MinK ($p < 0.01$, n = 16–42 cells). Human MiRP1 caused a 2-fold slowing of both components of Kv2.1 deactivation at −40 mV ($p < 0.05$, n = 16–42 cells) whereas human MinK had no significant effects on the τvalues (τ_{slow}, ms: Kv2.1 alone, 119 ± 9; Kv2.1-hMinK, 106 ± 7; Kv2.1-hMiRP1, 208 ± 20; τ_{fast}, ms: Kv2.1 alone, 17 ± 1; Kv2.1-MinK, 16 ± 1; Kv2.1-hMiRP1, 32 ± 2) (Figure 3F, G). Human MinK produced a small but statistically significant ($p < 0.05$) increase in the relative

amplitude of the slow component of deactivation whereas hMiRP1 had no significant effect on amplitude (Kv2.1 alone, 0.49 ± 0.02; Kv2.1-hMinK, 0.58 ± 0.04; Kv2.1-hMiRP1, 0.43 ± 0.04; n = 16–42 cells; Figure 3H). Despite their effects on Kv2.1 gating, neither rat MinK nor human MiRP1 significantly altered the sensitivity of Kv2.1 to block by TEA (Supplementary Figure 2).

Inherited LQTS mutations D76N and S74L alter MinK-Kv2.1 function

Human MinK variants D76N and S74L are associated with inherited LQTS, and both reduce MinK-KCNQ1 (I_{Ks}) current density by a combination of gating effects and reduced unitary conductance (Sesti & Goldstein, 1998; Splawski et al., 1997). Here, D76N-hMinK-Kv2.1 channels showed significantly reduced current density compared to wild-type hMinK-Kv2.1 complexes, while the apparent reduction observed with S74L-MinK did not reach statistical significance (D76N-MinK-Kv2.1, 332 ± 104 A/F; S74L-MinK-Kv2.1, 708 ± 73 A/F; *versus* hMinK-Kv2.1, 1022 ± 150 A/F) (Figure 4A, B). Neither mutation altered the voltage dependence or rate of hMinK-Kv2.1 activation (Figure 4C, D). Both mutations significantly increased the τof both components of deactivation but decreased the relative amplitude of the slow component (Figure 4E, F) without significantly altering inactivation (not shown).

Inherited LQTS mutations I57T and M54T impair MiRP1-Kv2.1 activation

Human MiRP1 variants M54T and I57T are associated with inherited and acquired LQTS; M54T accelerates MiRP1-hERG deactivation while I57T reduces MiRP1-hERG current density (Abbott et al., 1999; Sesti et al., 2000). Here, neither variant reduced mean current density of hMiRP1-Kv2.1 channels (M54T, 730± 89 A/F; I57T, 859 ± 100 A/F versus wild-type hMiRP1-Kv2.1, 846 ± 120 A/F) (Figure 5A, B). M54T positively shifted the voltage dependence of MiRP1-Kv2.1 channels by 9 mV ($V_{1/2\ activation}$ for M54T was 10.4 ± 1.1 mV versus 1.1 ± 0.4 mV for wild-type MiRP1-Kv2.1) whereas I57T had no significant effect ($V_{1/2\ activation}$ −0.6 ± 0.8 mV) (Figure 5C).

The most prominent effect of the MiRP1 mutations was a slowing of hMiRP1-Kv2.1 activation (Figure 5A, D). At all depolarizing voltages, the slowing of activation observed with wild-type hMiRP1 was significantly increased, with the M54T mutation having the greatest effect (wild-type hMiRP1, 10.0 ± 1.1 ms; I57T, 16.8 ± 2.0 ms; M54T, 50.2 ± 5.9 ms at +60 mV) (Figure 5E). Neither mutant altered MiRP1-Kv2.1 deactivation kinetics (both the τ and the relative amplitudes of the slow or fast components were unaltered, Figure 5F, G). Although wild-type MiRP1 did not alter Kv2.1 inactivation, there was a statistically significant reduction in the extent of inactivation by M54T (14.9 ± 1.7 % over 1 s) when compared to Kv2.1 homomers (28.8 ± 2.2 %, $p < 0.001$), wild-type MiRP1-Kv2.1 (23.4 ± 3.9 % $p < 0.05$) or I57T-MiRP1-Kv2.1 channels (23.9 ±2.1 % $p < 0.05$) (Figure 5H).

DISCUSSION

Multiple roles for MinK and MiRP1 in mammalian heart

The finding here that MinK and MiRP1 co-assemble with Kv2.1 αsubunits in rat heart, broaden the possible role of these two *KCNE* subunits in mammalian cardiac physiology. It has long been recognized that MinK-KCNQ1 complexes form I_{Ks} in mammalian heart (Barhanin et al., 1996; Sanguinetti et al., 1996). Since this discovery, MinK and MiRPs have been found to interact with a wide array of Kv channel α subunits expressed in the heart, although formation of native complexes has not been proven for all putative partnerships. Both MinK and MiRP1 are expressed in guinea pig, horse and human heart (Abbott et al., 1999; Bertaso et al., 2002; Jiang et al., 2004; Pereon et al., 2000). Our current findings for expression of MinK and MiRP1 in rat heart are consistent with previous reports showing that mRNA for both MinK (Folander et al., 1990; Ohya et al., 2002; Yang et al., 1994) and MiRP1 (Ohya et al., 2002) are expressed

in rat heart. Aside from KCNQ1, MinK also modulates ERG (McDonald et al., 1997), and although this association has not been established in human tissue, MinK-ERG complexes were found using co-immunoprecipitation studies in equine heart (Finley et al., 2002) and here in rat heart (Figure 1F). We also previously reported that *Xenopus laevis* MinK slows Kv2.1 activation in *Xenopus* oocytes (Gordon, Roepke & Abbott, 2006).

Using a *kcne2* null mouse line, we recently found that MiRP1 forms complexes with Kv1.5 and with Kv4.2 in adult murine ventricles, but not with Kv2.1 (Roepke et al., 2008). Native current recordings supported these findings, and together with our present data, demonstrate that expression in a tissue of two subunits capable of interaction does not necessarily confirm their native interaction. Likewise, in the present study we found that despite expression in rat heart, MiRP2 does not form stable complexes with Kv2.1 in rat heart, contrasting with our previous finding that MiRP2 forms stable complexes with Kv2.1 in rat brain (McCrossan et al., 2003). Further, the contrasting findings in the rat and mouse heart highlight the necessity to understand the limitations of studying a single model system, although we have yet to study murine atria, thus it is possible that MiRP1-Kv2.1 complexes exist there.

MiRP1 modulates hERG function and pharmacology, and MiRP1-hERG complexes may contribute to generating I_{Kr} in human heart (Abbott et al., 1999). Throughout rat heart development MiRP1 strongly co-localizes with rERG (Chun et al., 2004), consistent with our data here suggesting formation of MiRP1-rERG complexes in rat heart (Figure 1F). Further, in a canine model of cardiac disease, MiRP1 upregulation was recently shown to reduce I_{Kr} (Jiang et al., 2004), as would be expected if the two co-assemble in canine heart, because MiRP1 lowers the unitary conductance of ERG (Abbott et al., 1999). MiRP2 also suppresses hERG currents in *Xenopus* oocyte expression experiments (Abbott et al., 2001; Anantharam et al., 2003; Han et al., 2002; Lewis, McCrossan & Abbott, 2004; McCrossan et al., 2003; Schroeder et al., 2000). While the expression of MiRP2 in heart tissue suggests a role in cardiac excitability, it is not yet known whether MiRP2 modulates hERG, KCNQ1 or any other channels *in vivo* in mammalian heart.

Cardiac effects of genetic disruption of MinK and MiRP1

Cardiac expression, demonstration of the ability to modulate specific cardiac channels in heterologous systems, and native cardiac co-immunoprecipitations, all offer evidence supporting specific roles for MinK and MiRP1 in cardiac physiology. Genetic evidence provides perhaps stronger evidence in support of roles for MinK and MiRP1 in the heart, but what can it tell us about specific partnerships? MinK knockout was previously reported to induce only a mild cardiac phenotype (Charpentier et al., 1998), but the profound sensorineural deafness exhibited by MinK null mice (and KCNQ1 null mice) (Lee et al., 2000; Vetter et al., 1996) is consistent with association of MinK mutations with Jervell Lange-Nielsen syndrome (JLNS), an inherited human disorder that presents as LQTS and deafness (Splawski et al., 1997; Tyson et al., 1997). The disruption of potassium secretion into the endolymph of the inner ear in JLNS by knockout or mutation of MinK is accepted to be due to dysfunction of MinK-KCNQ1 complexes in the ear, especially as KCNQ1 mutations can also cause JLNS (Schulze-Bahr et al., 1997; Tyson et al., 1997), but the LQTS component could be also caused by dysfunction of other channels that MinK may associate with in the heart, including ERG (Bianchi et al., 1999; McDonald et al., 1997). Recently, MinK null mice were also found to exhibit atrial fibrillation (Temple et al., 2005), and a MinK polymorphism was previously found to be enriched in human atrial fibrillation patients compared to control subjects (Lai et al., 2002). Despite the fact that MinK increases KCNQ1 unitary and macroscopic conductance ~4-fold, MinK knockout increased I_K current in atrial myocytes; interestingly, this was not exclusively due to upregulation of currents sensitive to chromanol 293, a KCNQ1 and I_{Ks} blocker (Temple et al., 2005). Our present findings provide a possible molecular explanation

for this: if MinK-Kv2.1 currents form in murine atrium as they do in rat heart, then MinK knockout would be expected to upregulate atrial I_K (provided mouse MinK, like rat MinK, reduces Kv2.1 current density). Our present study in rat heart might also help explain the previously-observed heterogeneity in Kv2.1 current magnitude and kinetics isolated from the mid-myocardial left ventricular wall (Schultz, Volk & Ehmke, 2001). There, the authors speculate that heteromultimerization with other Kv channel α subunits might be a contributing factor; given our results, MinK and MiRP1 interaction should also be considered.

The effects reported here of D76N on human MinK-Kv2.1 function raise the possibility that disruption of MinK-Kv2.1 currents may contribute to D76N-associated disease - the combined effects of the D76N mutation serve to decrease the repolarizing ability of MinK-Kv2.1 complexes, predicted to lengthen the action potential in myocytes in which Kv2.1 is a repolarizing current. The single significant effect of S74L - slowing of hMinK-Kv2.1 deactivation, in contrast, could shorten the action potential by delaying channel closure toward the end of phase 3. However, while Kv2.1 is expressed in human heart, its role in human cardiac repolarization is not yet known, and its expression is likely much lower in human heart than that of hERG and KCNQ1 and therefore its role in human cardiac repolarization correspondingly less important.

Mutations and polymorphisms in MiRP1, including M54T and I57T, reduce MiRP1-hERG currents and are associated with inherited and drug-induced LQTS (Abbott et al., 1999; Isbrandt et al., 2002; Sesti et al., 2000). The R27C variant of MiRP1 is also implicated in atrial fibrillation, and shown to increase MiRP1-KCNQ1 currents without affecting MiRP1-hERG or MiRP1-HCN channel function (Yang et al., 2004). M54T and I57T produced reductions of 34–47% in MiRP1-hERG tail current density at −40 mV; M54T-MiRP1-hERG channels activated less readily at a given voltage and deactivated more rapidly than channels formed with wild-type MiRP1 and hERG (Abbott et al., 1999; Sesti et al., 2000). The effects of M54T and I57T on MiRP1-Kv2.1 channels found here – greatly slowed activation and (in the case of M54T) positively-shifted voltage dependence of activation – would also be expected to lengthen the action potential of cells requiring MiRP1-Kv2.1 for repolarization. Without a known role for Kv2.1 in human myocytes we cannot speculate further on the potential role of MiRP1-Kv2.1 current disruption in human cardiac pathophysiology. In mice, *kcne2* knockout prolongs ventricular action potential duration and increases the QT interval under sevoflurane anesthesia, but these effects are almost certainly due to reduced $I_{K,slow1}$ and $I_{to,f}$ density due to loss of MiRP1 regulation of Kv1.5 and Kv4.2, respectively (Roepke et al., 2008).

Conclusions and limitations

In summary, our data provide evidence for the presence of two novel potassium channel complexes in rat hearts, suggesting a role for MinK-Kv2.1 and MiRP1-Kv2.1 complexes in cardiac physiology. Both MinK and MiRP1 alter Kv2.1 function; mutations in MinK and MiRP1 associated with human LQTS impair function of complexes formed with Kv2.1. Further studies are necessary to determine exactly when and where in the heart these complexes form, and how important regulation of Kv2.1 by MinK or MiRP1 is to the generation of I_K in the hearts of rats and other species. These studies may be hampered if the lack of effect of MinK or MiRP1 on Kv2.1 sensitivity to TEA is also observed with other pharmacological tools, and ultimately a combination of genetic evidence and regional native electrophysiology studies may be necessary to pin down roles for MinK-Kv2.1 and MiRP1-Kv2.1 complexes in specific cardiac regions or cell-types. Further studies are also required to determine which of the sequence differences between the rat and human forms of MinK and MiRP1 (29/129 and 22/123 residues, respectively) give rise to their functional differences. No obvious patterns emerge from examination of these sequences, except that the transmembrane domains differ

the least between rat and human in each case (1–2 residues), with the rest of the variant residues scattered throughout the extracellular and intracellular domains (Abbott & Goldstein, 1998).

An extensive diversity of Kv channel subunit expression has been identified between atria and ventricles, and Kv channel subunits are also differentially expressed in circumscribed regions in the left ventricular wall, between endo- and epicardial regions, and in distinct areas of the conduction system as well as in the aging and diseased heart (Dixon & McKinnon, 1994; Jiang et al., 2004; Pourrier et al., 2003; Schultz et al., 2001). Kv2.1 is highly expressed in rat heart atria and to a lesser extent in rat ventricles; MinK and MiRP1 are expressed in rat heart (Figure 1), murine atria and SA and AV nodes, and in human, horse and guinea pig atria and ventricles (Barry et al., 1995; Finley et al., 2002; Jiang et al., 2004; Szabo et al., 2005; Warth & Barhanin, 2002). Additionally MiRP1 expression is up-regulated in aging and down-regulated in ischemic rat hearts (Jiang et al., 2004) and both MinK and MiRP1 are reportedly highly expressed in canine purkinje fibers (Pourrier et al., 2003).

It becomes apparent that the task of identifying specific MiRP-α subunit partnerships and their native current correlates is a monumental one that will require concerted biochemical, pharmacological and genetic analyses at the sub-tissue level in a range of species; the present study essentially offers a starting point for analysis of Kv2.1 complexes. This task may ultimately prove futile in some cases if MiRPs provide a mechanism for dynamically modulating channel function as opposed to providing an expanded but defined range of currents in combination with a finite amount of different α subunits. We previously found that interactions of MinK, MiRP1 and MiRP2 increase functional diversity of the Kv3 α subunit family, broadening its potential role outside that of sustaining rapid firing in neurons (Lewis et al., 2004) and we now find that Kv2.1 is also differentially modulated by MinK, MiRP1 and (previously) MiRP2 (McCrossan et al., 2003), but we are no closer to understanding exactly how all these possible combinations are utilized in native tissue. A recent quantitative RT-PCR analysis showed differential mRNA expression for all 5 MiRPs across the right and left atria and ventricles of human heart, and increased expression in cardiomyopathy (Lundquist et al., 2005). In the same study, CHO cell expression experiments showed that MinK prevented modulation of KCNQ1 by MiRP1, but that MiRPs 2–4 could override effects of MinK on KCNQ1–thus KCNQ1 may be modulated by multiple MiRPs in human heart depending on sub-tissue or even subcellular distribution and other temporal or regulatory factors. Now we understand that both MiRPs and α subunits exhibit promiscuous partnering, future studies are warranted to examine how spatial and temporal variation in cardiac expression levels of MiRPs and Kv channel α subunits impacts complex formation, native current properties, and action potential duration and refractoriness in different regions of the heart in man and in animal models.

Supplementary Material

Refer to Web version on PubMed Central for supplementary material.

Acknowledgments

This work was supported by the NIH (R01 HL079275 to G.W.A). We are grateful to Dr. Sandra Chaplan for assistance with antibody development, and to Dr. Daniel J. Lerner for insightful comments on the manuscript.

Abbreviations

ERG	*ether-a-go-go* related gene product
Kv channel	voltage-gated potassium channel

MiRP	MinK-Related Peptide
TEA	tetraethylammonium
TM	transmembrane

References

Abbott GW, Butler MH, Bendahhou S, Dalakas MC, Ptacek LJ, Goldstein SA. MiRP2 forms potassium channels in skeletal muscle with Kv3.4 and is associated with periodic paralysis. Cell 2001;104:217–31. [PubMed: 11207363]

Abbott GW, Goldstein SA. A superfamily of small potassium channel subunits: form and function of the MinK-related peptides (MiRPs). Q Rev Biophys 1998;31:357–98. [PubMed: 10709243]

Abbott GW, Sesti F, Splawski I, Buck ME, Lehmann MH, Timothy KW, Keating MT, Goldstein SA. MiRP1 Forms IKr Potassium Channels with HERG and Is Associated with Cardiac Arrhythmia. Cell 1999;97:175–187. [PubMed: 10219239]

Anantharam A, Lewis A, Panaghie G, Gordon E, McCrossan ZA, Lerner DJ, Abbott GW. RNA Interference Reveals That Endogenous Xenopus MinK-related Peptides Govern Mammalian K+ Channel Function in Oocyte Expression Studies. J Biol Chem 2003;278:11739–45. [PubMed: 12529362]

Antonucci DE, Lim ST, Vassanelli S, Trimmer JS. Dynamic localization and clustering of dendritic Kv2.1 voltage-dependent potassium channels in developing hippocampal neurons. Neuroscience 2001;108:69–81. [PubMed: 11738132]

Barhanin J, Lesage F, Guillemare E, Fink M, Lazdunski M, Romey G. K(V)LQT1 and lsK (minK) proteins associate to form the I(Ks) cardiac potassium current. Nature 1996;384:78–80. [PubMed: 8900282]

Barry DM, Trimmer JS, Merlie JP, Nerbonne JM. Differential expression of voltage-gated K+ channel subunits in adult rat heart. Relation to functional K+ channels? Circ Res 1995;77:361–9. [PubMed: 7614722]

Bertaso F, Sharpe CC, Hendry BM, James AF. Expression of voltage-gated K+ channels in human atrium. Basic Res Cardiol 2002;97:424–33. [PubMed: 12395204]

Bianchi L, Shen Z, Dennis AT, Priori SG, Napolitano C, Ronchetti E, Bryskin R, Schwartz PJ, Brown AM. Cellular dysfunction of LQT5-minK mutants: abnormalities of IKs, IKr and trafficking in long QT syndrome. Hum Mol Genet 1999;8:1499–507. [PubMed: 10400998]

Bou-Abboud E, Li H, Nerbonne JM. Molecular diversity of the repolarizing voltage-gated K+ currents in mouse atrial cells. J Physiol 2000;529(Pt 2):345–58. [PubMed: 11101645]

Bou-Abboud E, Nerbonne JM. Molecular correlates of the calcium-independent, depolarization-activated K+ currents in rat atrial myocytes. J Physiol 1999;517(Pt 2):407–20. [PubMed: 10332091]

Capuano V, Ruchon Y, Antoine S, Sant MC, Renaud JF. Ventricular hypertrophy induced by mineralocorticoid treatment or aortic stenosis differentially regulates the expression of cardiac K+ channels in the rat. Mol Cell Biochem 2002;237:1–10. [PubMed: 12236575]

Charpentier F, Merot J, Riochet D, Le Marec H, Escande D. Adult KCNE1-knockout mice exhibit a mild cardiac cellular phenotype. Biochem Biophys Res Commun 1998;251:806–10. [PubMed: 9790991]

Chen YH, Xu SJ, Bendahhou S, Wang XL, Wang Y, Xu WY, Jin HW, Sun H, Su XY, Zhuang QN, Yang YQ, Li YB, Liu Y, Xu HJ, Li XF, Ma N, Mou CP, Chen Z, Barhanin J, Huang W. KCNQ1 gain-of-function mutation in familial atrial fibrillation. Science 2003;299:251–4. [PubMed: 12522251]

Chun KR, Koenen M, Katus HA, Zehelein J. Expression of the IKr components KCNH2 (rERG) and KCNE2 (rMiRP1) during late rat heart development. Exp Mol Med 2004;36:367–371. [PubMed: 15365256]

Conforti L, Millhorn DE. Selective inhibition of a slow-inactivating voltage-dependent K+ channel in rat PC12 cells by hypoxia. J Physiol 1997;502(Pt 2):293–305. [PubMed: 9263911]

Dixon JE, McKinnon D. Quantitative analysis of potassium channel mRNA expression in atrial and ventricular muscle of rats. Circ Res 1994;75:252–60. [PubMed: 8033339]

Du J, Tao-Cheng JH, Zerfas P, McBain CJ. The K+ channel, Kv2.1, is apposed to astrocytic processes and is associated with inhibitory postsynaptic membranes in hippocampal and cortical principal neurons and inhibitory interneurons. Neuroscience 1998;84:37–48. [PubMed: 9522360]

Finley MR, Li Y, Hua F, Lillich J, Mitchell KE, Ganta S, Gilmour RF Jr, Freeman LC. Expression and coassociation of ERG1, KCNQ1, and KCNE1 potassium channel proteins in horse heart. Am J Physiol Heart Circ Physiol 2002;283:H126–38. [PubMed: 12063283]

Folander K, Smith JS, Antanavage J, Bennett C, Stein RB, Swanson R. Cloning and expression of the delayed-rectifier IsK channel from neonatal rat heart and diethylstilbestrol-primed rat uterus. Proc Natl Acad Sci U S A 1990;87:2975–9. [PubMed: 2183220]

Frech GC, VanDongen AM, Schuster G, Brown AM, Joho RH. A novel potassium channel with delayed rectifier properties isolated from rat brain by expression cloning. Nature 1989;340:642–5. [PubMed: 2770868]

Gordon E, Roepke TK, Abbott GW. Endogenous KCNE subunits govern Kv2.1 K+ channel activation kinetics in Xenopus oocyte studies. Biophys J 2006;90:1223–31. [PubMed: 16326911]

Han W, Bao W, Wang Z, Nattel S. Comparison of ion-channel subunit expression in canine cardiac Purkinje fibers and ventricular muscle. Circ Res 2002;91:790–7. [PubMed: 12411393]

Huang B, Qin D, El-Sherif N. Spatial alterations of Kv channels expression and K(+) currents in post-MI remodeled rat heart. Cardiovasc Res 2001;52:246–54. [PubMed: 11684072]

Isbrandt D, Friederich P, Solth A, Haverkamp W, Ebneth A, Borggrefe M, Funke H, Sauter K, Breithardt G, Pongs O, Schulze-Bahr E. Identification and functional characterization of a novel KCNE2 (MiRP1) mutation that alters HERG channel kinetics. J Mol Med 2002;80:524–32. [PubMed: 12185453]

Jiang M, Zhang M, Tang DG, Clemo HF, Liu J, Holwitt D, Kasirajan V, Pond AL, Wettwer E, Tseng GN. KCNE2 protein is expressed in ventricles of different species, and changes in its expression contribute to electrical remodeling in diseased hearts. Circulation 2004;109:1783–8. [PubMed: 15066947]

Kaab S, Dixon J, Duc J, Ashen D, Nabauer M, Beuckelmann DJ, Steinbeck G, McKinnon D, Tomaselli GF. Molecular basis of transient outward potassium current downregulation in human heart failure: a decrease in Kv4.3 mRNA correlates with a reduction in current density. Circulation 1998;98:1383–93. [PubMed: 9760292]

Kuryshev YA, Gudz TI, Brown AM, Wible BA. KChAP as a chaperone for specific K(+) channels. Am J Physiol Cell Physiol 2000;278:C931–41. [PubMed: 10794667]

Lai LP, Su MJ, Yeh HM, Lin JL, Chiang FT, Hwang JJ, Hsu KL, Tseng CD, Lien WP, Tseng YZ, Huang SK. Association of the human minK gene 38G allele with atrial fibrillation: Evidence of possible genetic control on the pathogenesis of atrial fibrillation. Am Heart J 2002;144:485–90. [PubMed: 12228786]

Le Bouter S, Demolombe S, Chambellan A, Bellocq C, Aimond F, Toumaniantz G, Lande G, Siavoshian S, Baro I, Pond AL, Nerbonne JM, Leger JJ, Escande D, Charpentier F. Microarray analysis reveals complex remodeling of cardiac ion channel expression with altered thyroid status: relation to cellular and integrated electrophysiology. Circ Res 2003;92:234–42. [PubMed: 12574152]

Lee MP, Ravenel JD, Hu RJ, Lustig LR, Tomaselli G, Berger RD, Brandenburg SA, Litzi TJ, Bunton TE, Limb C, Francis H, Gorelikow M, Gu H, Washington K, Argani P, Goldenring JR, Coffey RJ, Feinberg AP. Targeted disruption of the Kvlqt1 gene causes deafness and gastric hyperplasia in mice. J Clin Invest 2000;106:1447–55. [PubMed: 11120752]

Lewis A, McCrossan ZA, Abbott GW. MinK, MiRP1 and MiRP2 diversify Kv3.1 and Kv3.2 potassium channel gating. J Biol Chem 2004;279:2884–92.

Lundquist AL, Manderfield LJ, Vanoye CG, Rogers CS, Donahue BS, Chang PA, Drinkwater DC, Murray KT, George AL Jr. Expression of multiple KCNE genes in human heart may enable variable modulation of I(Ks). J Mol Cell Cardiol 2005;38:277–87. [PubMed: 15698834]

McCrossan ZA, Abbott GW. The MinK-Related Peptides. Neuropharmacology 2004;47:787–821. [PubMed: 15527815]

McCrossan ZA, Lewis A, Panaghie G, Jordan PN, Christini DJ, Lerner DJ, Abbott GW. MinK-related peptide 2 modulates Kv2.1 and Kv3.1 potassium channels in mammalian brain. J Neurosci 2003;23:8077–91. [PubMed: 12954870]

McDonald TV, Yu Z, Ming Z, Palma E, Meyers MB, Wang KW, Goldstein SA, Fishman GI. A minK-HERG complex regulates the cardiac potassium current I(Kr). Nature 1997;388:289–92. [PubMed: 9230439]

Murakoshi H, Trimmer JS. Identification of the Kv2.1 K+ channel as a major component of the delayed rectifier K+ current in rat hippocampal neurons. J Neurosci 1999;19:1728–35. [PubMed: 10024359]

Ohya S, Asakura K, Muraki K, Watanabe M, Imaizumi Y. Molecular and functional characterization of ERG, KCNQ, and KCNE subtypes in rat stomach smooth muscle. Am J Physiol Gastrointest Liver Physiol 2002;282:G277–87. [PubMed: 11804849]

Pereon Y, Demolombe S, Baro I, Drouin E, Charpentier F, Escande D. Differential expression of KvLQT1 isoforms across the human ventricular wall. Am J Physiol Heart Circ Physiol 2000;278:H1908–15. [PubMed: 10843888]

Piccini M, Vitelli F, Seri M, Galietta LJ, Moran O, Bulfone A, Banfi S, Pober B, Renieri A. KCNE1-like gene is deleted in AMME contiguous gene syndrome: identification and characterization of the human and mouse homologs. Genomics 1999;60:251–7. [PubMed: 10493825]

Pitts BJ. Stoichiometry of sodium-calcium exchange in cardiac sarcolemmal vesicles. Coupling to the sodium pump. J Biol Chem 1979;254:6232–5. [PubMed: 447709]

Post MA, Kirsch GE, Brown AM. Kv2.1 and electrically silent Kv6.1 potassium channel subunits combine and express a novel current. FEBS Lett 1996;399:177–82. [PubMed: 8980147]

Pourrier M, Zicha S, Ehrlich J, Han W, Nattel S. Canine ventricular KCNE2 expression resides predominantly in purkinje fibers. Circulation Research 2003;93:189–191. [PubMed: 12842918]

Roepke TK, Kontogeorgis A, Ovanez C, Xu X, Young JB, Purtell K, Goldstein PA, Christini DJ, Peters NS, Akar FG, Gutstein DE, Lerner DJ, Abbott GW. Targeted deletion of kcne2 impairs ventricular repolarization via disruption of I(K,slow1) and I(to,f). Faseb J 2008;22:3648–60. [PubMed: 18603586]

Salinas M, de Weille J, Guillemare E, Lazdunski M, Hugnot JP. Modes of regulation of shab K+ channel activity by the Kv8.1 subunit. J Biol Chem 1997;272:8774–80. [PubMed: 9079713]

Salinas M, Duprat F, Heurteaux C, Hugnot JP, Lazdunski M. New modulatory alpha subunits for mammalian Shab K+ channels. J Biol Chem 1997;272:24371–9. [PubMed: 9305895]

Sanguinetti MC, Curran ME, Zou A, Shen J, Spector PS, Atkinson DL, Keating MT. Coassembly of K(V)LQT1 and minK (IsK) proteins to form cardiac I(Ks) potassium channel. Nature 1996;384:80–3. [PubMed: 8900283]

Schroeder BC, Waldegger S, Fehr S, Bleich M, Warth R, Greger R, Jentsch TJ. A constitutively open potassium channel formed by KCNQ1 and KCNE3. Nature 2000;403:196–9. [PubMed: 10646604]

Schultz JH, Volk T, Ehmke H. Heterogeneity of Kv2.1 mRNA expression and delayed rectifier current in single isolated myocytes from rat left ventricle. Circ Res 2001;88:483–90. [PubMed: 11249871]

Schulze-Bahr E, Haverkamp W, Wedekind H, Rubie C, Hordt M, Borggrefe M, Assmann G, Breithardt G, Funke H. Autosomal recessive long-QT syndrome (Jervell Lange-Nielsen syndrome) is genetically heterogeneous. Hum Genet 1997;100:573–6. [PubMed: 9341873]

Sesti F, Abbott GW, Wei J, Murray KT, Saksena S, Schwartz PJ, Priori SG, Roden DM, George AL Jr, Goldstein SA. A common polymorphism associated with antibiotic-induced cardiac arrhythmia. Proc Natl Acad Sci U S A 2000;97:10613–8. [PubMed: 10984545]

Sesti F, Goldstein SA. Single-channel characteristics of wild-type IKs channels and channels formed with two minK mutants that cause long QT syndrome. J Gen Physiol 1998;112:651–63. [PubMed: 9834138]

Splawski I, Timothy KW, Vincent GM, Atkinson DL, Keating MT. Molecular basis of the long-QT syndrome associated with deafness. N Engl J Med 1997;336:1562–7. [PubMed: 9164812]

Splawski I, Tristani-Firouzi M, Lehmann MH, Sanguinetti MC, Keating MT. Mutations in the hminK gene cause long QT syndrome and suppress IKs function. Nat Genet 1997;17:338–40. [PubMed: 9354802]

Szabo G, Szentandrassy N, Biro T, Toth BI, Czifra G, Magyar J, Banyasz T, Varro A, Kovacs L, Nanasi PP. Asymmetrical distribution of ion channels in canine and human left-ventricular wall: epicardium versus midmyocardium. Pflugers Arch. 2005

Temple J, Frias P, Rottman J, Yang T, Wu Y, Verheijck EE, Zhang W, Siprachanh C, Kanki H, Atkinson JB, King P, Anderson ME, Kupershmidt S, Roden DM. Atrial Fibrillation in KCNE1-Null Mice. Circ Res 2005;97:62–9. [PubMed: 15947250]

Tyson J, Tranebjaerg L, Bellman S, Wren C, Taylor JF, Bathen J, Aslaksen B, Sorland SJ, Lund O, Malcolm S, Pembrey M, Bhattacharya S, Bitner-Glindzicz M. IsK and KvLQT1: mutation in either of the two subunits of the slow component of the delayed rectifier potassium channel can cause Jervell and Lange-Nielsen syndrome. Hum Mol Genet 1997;6:2179–85. [PubMed: 9328483]

Van Wagoner DR, Pond AL, McCarthy PM, Trimmer JS, Nerbonne JM. Outward K+ current densities and Kv1.5 expression are reduced in chronic human atrial fibrillation. Circ Res 1997;80:772–81. [PubMed: 9168779]

Vetter DE, Mann JR, Wangemann P, Liu J, McLaughlin KJ, Lesage F, Marcus DC, Lazdunski M, Heinemann SF, Barhanin J. Inner ear defects induced by null mutation of the isk gene. Neuron 1996;17:1251–64. [PubMed: 8982171]

Warth R, Barhanin J. The multifaceted phenotype of the knockout mouse for the KCNE1 potassium channel gene. Am J Physiol Regul Integr Comp Physiol 2002;282:R639–48. [PubMed: 11832382]

Xu C, Lu Y, Tang G, Wang R. Expression of voltage-dependent K(+) channel genes in mesenteric artery smooth muscle cells. Am J Physiol 1999;277:G1055–63. [PubMed: 10564112]

Xu H, Barry DM, Li H, Brunet S, Guo W, Nerbonne JM. Attenuation of the slow component of delayed rectification, action potential prolongation, and triggered activity in mice expressing a dominant-negative Kv2 alpha subunit. Circ Res 1999;85:623–33. [PubMed: 10506487]

Yang T, Wathen MS, Felipe A, Tamkun MM, Snyders DJ, Roden DM. K+ currents and K+ channel mRNA in cultured atrial cardiac myocytes (AT-1 cells). Circ Res 1994;75:870–8. [PubMed: 7923633]

Yang Y, Xia M, Jin Q, Bendahhou S, Shi J, Chen Y, Liang B, Lin J, Liu Y, Liu B, Zhou Q, Zhang D, Wang R, Ma N, Su X, Niu K, Pei Y, Xu W, Chen Z, Wan H, Cui J, Barhanin J, Chen Y. Identification of a KCNE2 gain-of-function mutation in patients with familial atrial fibrillation. Am J Hum Genet 2004;75:899–905. [PubMed: 15368194]

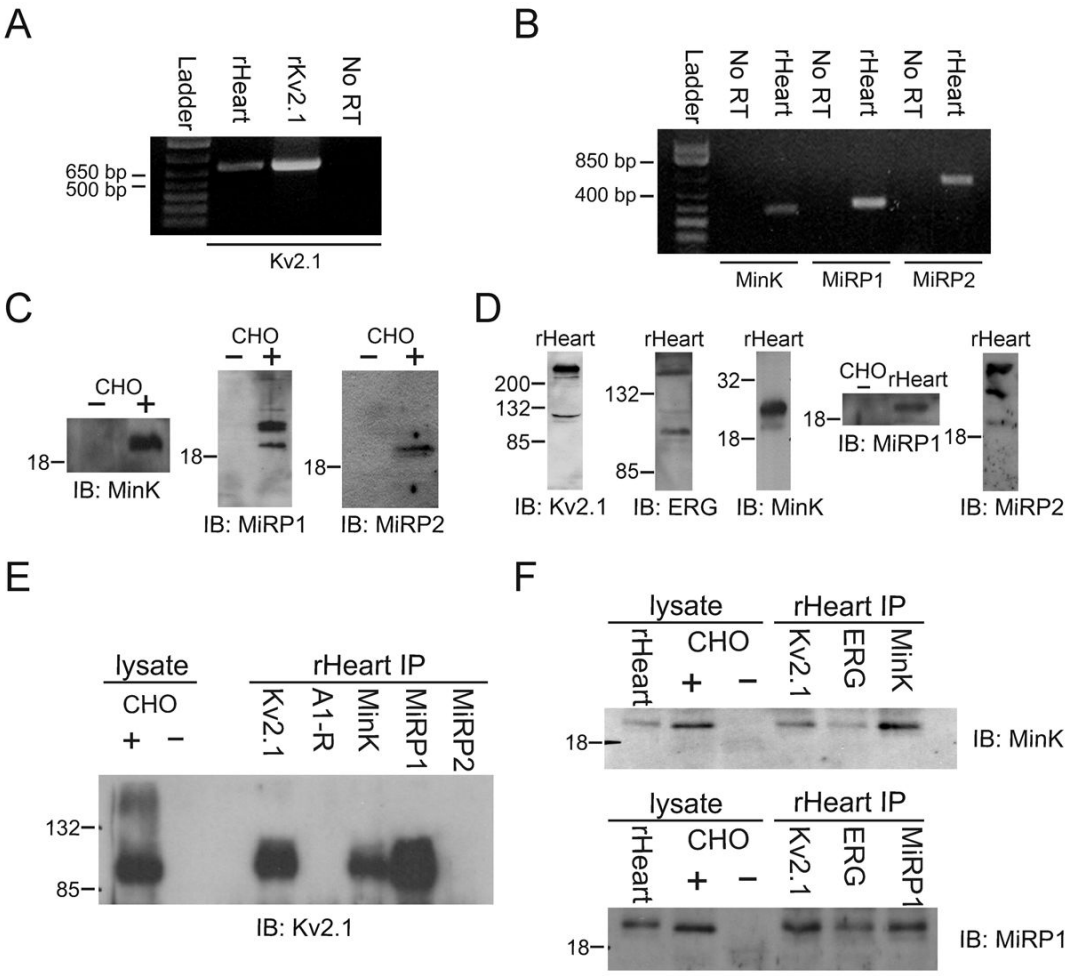

Figure 1. Immunoprecipitation of MinK-Kv2.1 and MiRP1-Kv2.1 complexes from rat heart

A. RT-PCR indicating expression of Kv2.1 mRNA in rat heart. Markers indicate migration of DNA ladder markers on agarose gel. mRNA was extracted from rat heart and then cDNA was produced by reverse transcription then amplified by Kv2.1-specific primers. Lanes: rHeart, cDNA amplified from rat heart mRNA; rKv2.1, positive control using Kv2.1 cDNA in a plasmid; No RT, as for rHeart lane but without reverse transcription (negative control).

B. RT-PCR showing expression of MinK, MiRP1 and MiRP2 mRNA in rat heart. Markers indicate migration of DNA ladder markers on agarose gel. Lanes: rHeart, cDNA amplified from rat heart mRNA with primers as indicated; No RT, as for rHeart lanes but without reverse transcription (negative controls).

C. Western blot analysis of MinK, MiRP1 and MiRP2 in CHO cells transfected with expression plasmids containing cDNA for MinK, MiRP1 or MiRP2, respectively. '−' indicates non-transfected CHO cell lysate (negative control); '+' indicates lysates from CHO cells transfected with MinK, MiRP1 or MiRP2, as indicated by the antibody used for immunoblotting ('IB', lower labels). Numbered labels to left of each blot indicate migration of molecular weight markers (in kD) on SDS-PAGE gel.

D. Western blot analysis of native channel subunit expression in rat heart membrane fractions. Lanes: '−' indicates non-transfected CHO cell lysate (negative control); 'rHeart' indicates membrane fraction from rat heart. Lower labels indicate antibody used for immunoblotting ('IB'). Numbered labels to left of each blot indicate migration of molecular weight markers (in kD) on SDS-PAGE gel.

E. Native co-immunoprecipitations of channel subunits from rat heart membrane fractions. Exemplar western blot using anti-Kv2.1 antibody for immunblotting ('IB') of Kv2.1 in Kv2.1-transfected CHO cell lysate, and in rat heart membrane fractions ('rHeart IP') immunoprecipitated by antibodies raised against Kv2.1, MinK or MiRP1 (n = 4 experiments). Kv2.1 was not detected in non-transfected CHO cell lysate or in rat heart membrane fractions immunoprecipitated by antibodies raised against the A1 adenosine receptor (A1-R) or MiRP2 (n = 2 experiments). Numbered labels to left of each blot indicate migration of molecular weight markers (in kD) on SDS-PAGE gel.

F. Reciprocal native co-immunoprecipitations of channel subunits from rat heart membrane fractions. Western blots using anti-MinK (upper gel) or anti-MiRP1 (lower gel) antibodies for immunoblotting ('IB'). MinK was present in rat heart membranes, MinK-transfected ('+') CHO cell lysate, and in rat heart membrane fractions ('rHeart IP') immunoprecipitated by antibodies raised against Kv2.1, MinK or ERG (n = 2 experiments). MiRP1 was present in rat heart membranes, MiRP1-transfected ('+') CHO cell lysate, and in rat heart membrane fractions ('rHeart IP') immunoprecipitated by antibodies raised against Kv2.1, MiRP1 or ERG (n = 2 experiments). Neither subunit was detected in non-transfected CHO cell lysate. Numbered labels to left of each blot indicate migration of molecular weight markers (in kD) on SDS-PAGE gel.

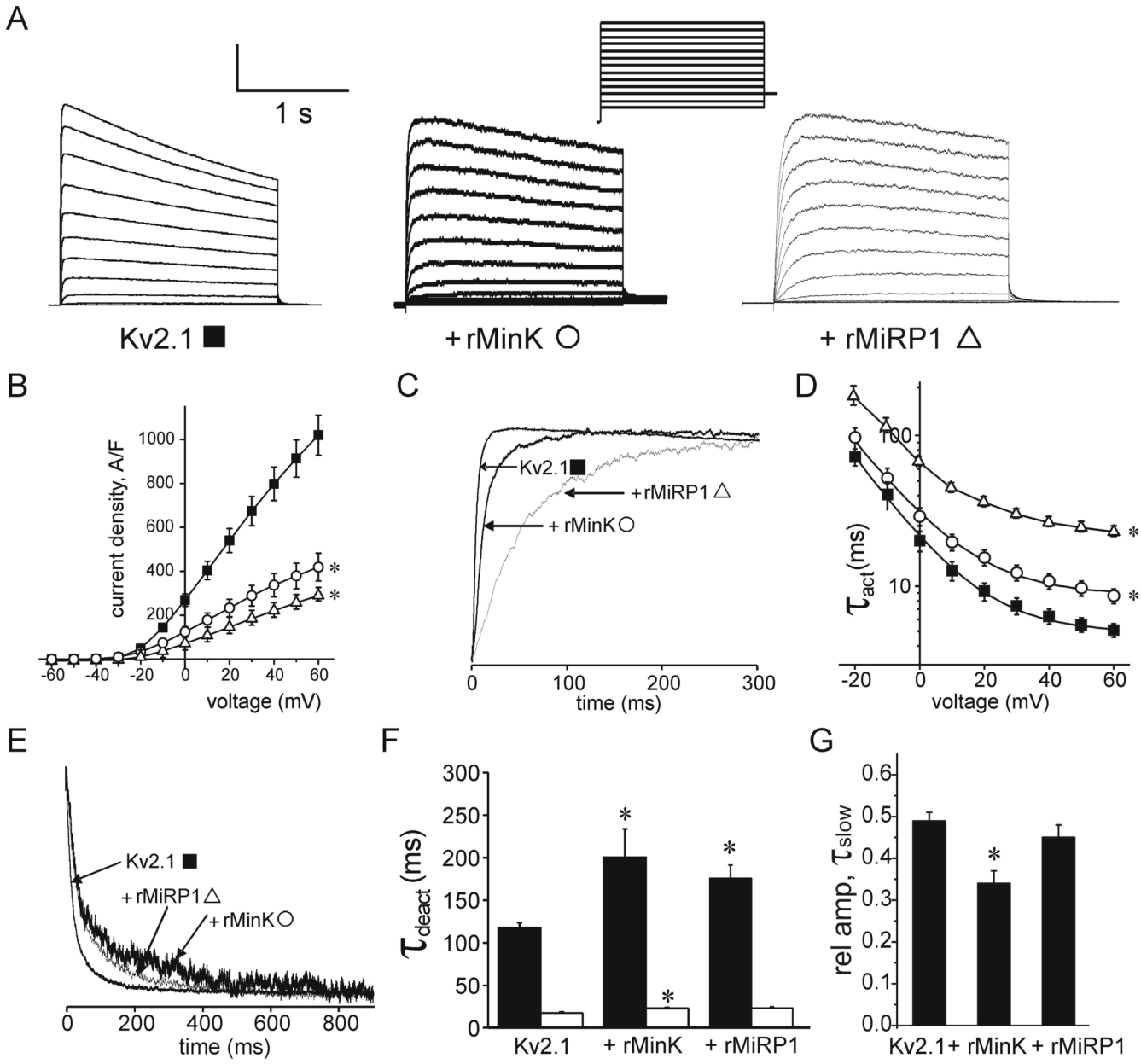

Figure 2. Modulation of Kv2.1 by rat MinK and MiRP1

A. Exemplar traces showing currents recorded from CHO cells transfected with Kv2.1 alone or co-transfected with rat MinK or MiRP1 as indicated. Insets: left, scale bars; right, voltage protocol. Vertical scale: 2nA, Kv2.1 and rMiRP1-Kv2.1; 0.5 nA, rMinK-Kv2.1.

B. Mean peak current density from CHO cells transfected with Kv2.1 alone (filled squares, $n = 61$), or co-transfected with rMinK (open circles, $n = 14$) or rMiRP1 (triangles, n = 17). * statistical significance versus Kv2.1 alone, $p < 0.05$.

C. Normalized exemplar traces showing expanded view of Kv2.1, rMinK-Kv2.1 and rMiRP1-Kv2.1 activation at 0 mV.

D. Mean activation rates of Kv2.1, rMinK-Kv2.1 and rMiRP1-Kv2.1 channels at activation voltages between −20 mV and +60 mV, fitted with a single exponential function, expressed as τ_{act}. * statistical significance versus Kv2.1 alone, $p < 0.05$. Cells and symbols as in panel B.

E. Normalized exemplar traces showing expanded view of Kv2.1, rMinK-Kv2.1 and rMiRP1-Kv2.1 deactivation at −40mV.

F. Mean deactivation rates of Kv2.1, rMinK-Kv2.1 and rMiRP1-Kv2.1 currents at −40mV fitted with a double exponential function, showing slow (black) and fast (white) τ_{deact} components. * statistical significance versus Kv2.1 alone, $p < 0.05$.

G. Mean fractional amplitude of the slow component of deactivation rates of Kv2.1, rMinK-Kv2.1 and rMiRP1-Kv2.1 currents at −40mV fitted with a double exponential function. * statistical significance versus Kv2.1 alone, $p < 0.05$.

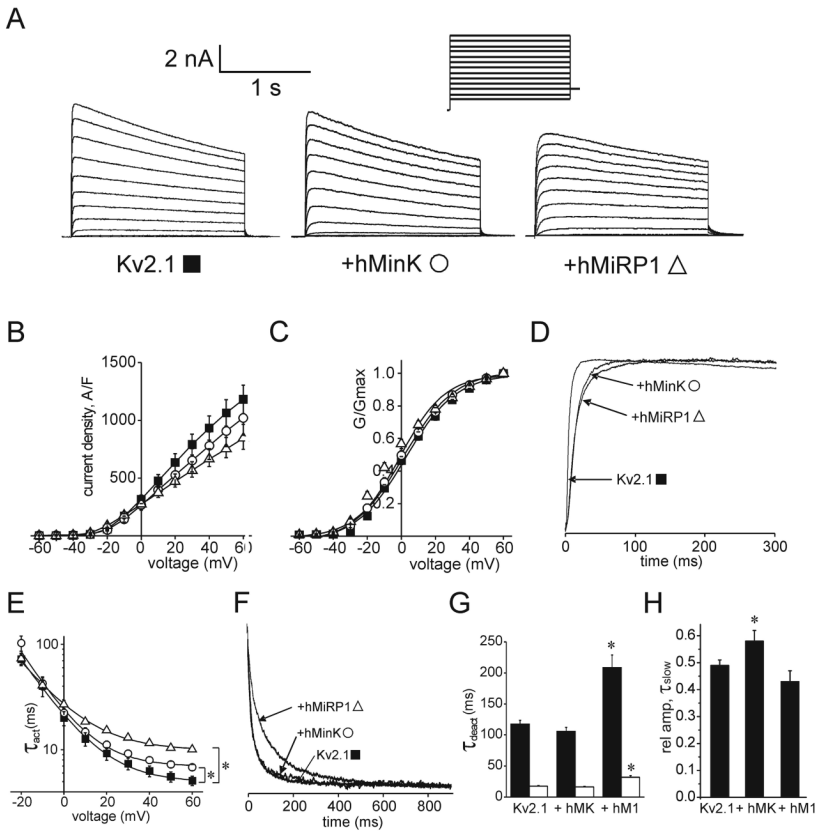

Figure 3. Human MinK and MiRP1 slow Kv2.1 gating

A. Exemplar traces showing currents recorded from CHO cells transfected with Kv2.1 alone or co-transfected with human MinK or MiRP1 as indicated. Insets: left, scale bars; right, voltage protocol.

B. Mean peak current density from CHO cells transfected with Kv2.1 alone (filled squares, $n = 42$), or co-transfected with hMinK (open circles, $n = 24$) or hMiRP1 (open triangles, $n = 16$).

C. Mean normalized conductance-voltage relationships, cells and symbols as in panel B. Data were fit with a Boltzman function, $G = G_{max}/[1 + \exp(V–V_{0.5}/k)]$, giving values for midpoint voltage dependence of activation of: Kv2.1, 4.4 ± 0.7 mV; MinK-Kv2.1, 1.0 ± 1.0 mV; MiRP1-Kv2.1, −0.6 ± 0.8 mV; slopes were 11.3 ± 0.4 mV, 15.2 ± 0.9 mV, and 13.1 ± 0.5 mV, respectively.

D. Normalized exemplar traces showing expanded view of Kv2.1, hMinK-Kv2.1 and hMiRP1-Kv2.1 activation at 0 mV.

E. Mean activation rates of Kv2.1, hMinK-Kv2.1 and hMiRP1-Kv2.1 channels at activation voltages between −10 mV and +60 mV, fitted with a single exponential function, expressed as τ_{act}.

F. Normalized exemplar traces showing expanded view of Kv2.1, hMinK-Kv2.1 and hMiRP1-Kv2.1 deactivation at −40mV.

G. Mean deactivation rates of Kv2.1, hMinK-Kv2.1 and hMiRP1-Kv2.1 currents at −40mV fitted with a double exponential function, showing slow (black) and fast (white) τ_{deact} components. * statistical significance versus Kv2.1 alone, $p < 0.05$.

H. Mean fractional amplitude of the slow component of deactivation rates of Kv2.1, hMinK-Kv2.1 and hMiRP1-Kv2.1 currents at −40mV fitted with a double exponential function. * statistical significance versus Kv2.1 alone, $p < 0.05$.

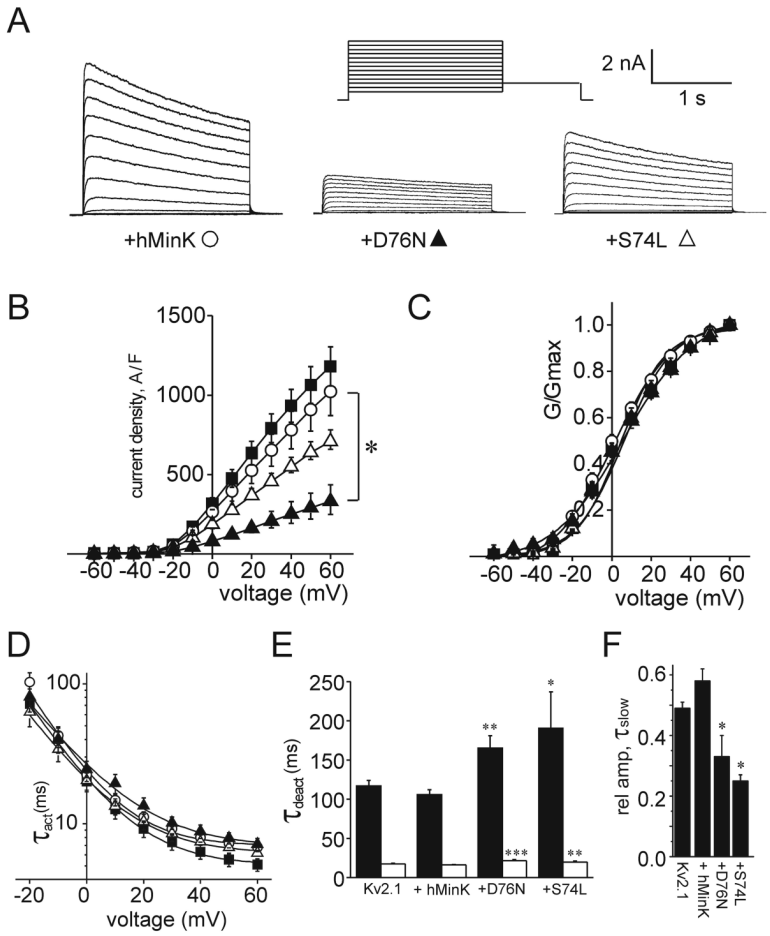

Figure 4. Effects of inherited human MinK mutations on MinK-Kv2.1 function

A. Exemplar traces showing currents recorded from CHO cells co-transfected with Kv2.1 + wild-type human MinK ('+hMinK'), Kv2.1 + D76N-MinK ('+D76N') or Kv2.1 + S74L-MinK ('+S74L'), as indicated. Insets: left, voltage protocol; right, scale bars.

B. Mean peak current density from CHO cells transfected with Kv2.1 alone (filled squares) or with wild-type (open circles, $n = 14$), D76N (filled triangles, $n = 9$) or S74L (open triangles, $n = 11$) human MinK. * statistically significant difference ($p < 0.001$).

C. Mean normalized conductance-voltage relationships, cells and symbols as in panel B. Fitting of the data with a Boltzman function, $G = G_{max}/[1 + \exp(V–V_{0.5}/k)]$, gave values for midpoint voltage dependence of activation of: Kv2.1, 4.4 ± 0.7 mV; wild-type human MinK-Kv2.1, 1.0 ± 1.0 mV; D76N-MinK-Kv2.1, 6.0 ± 1.6 mV; S74L-MinK-Kv2.1, 6.2 ± 0.7 mV; slopes were 11.3 ± 0.4, 15.2 ± 0.9, 18.0 ± 1.8, and 12.5 ± 0.5 mV, respectively.

D. Mean activation rates, cells and symbols as in panel B. Activation rates at voltages between −10 mV and +60 mV, were fitted with a single exponential function, expressed as τ_{act}.

E. Mean deactivation rates for cells as in panel B, subunits as indicated. Deactivation rates at −30 mV were fitted with a double exponential function, showing slow (black) and fast (white) τ_{deact} components. Asterisks denote statistically significant difference versus wild-type human MinK-MinK: *$p < 0.05$; **$p < 0.01$; *** $p < 0.001$.

F. Mean fractional amplitude of the slow component of deactivation rates of Kv2.1, and Kv2.1 with wild-type or mutant hMinK, currents at −40mV fitted with a double exponential function. * statistical significance versus Kv2.1 + wild-type MinK, $p < 0.05$.

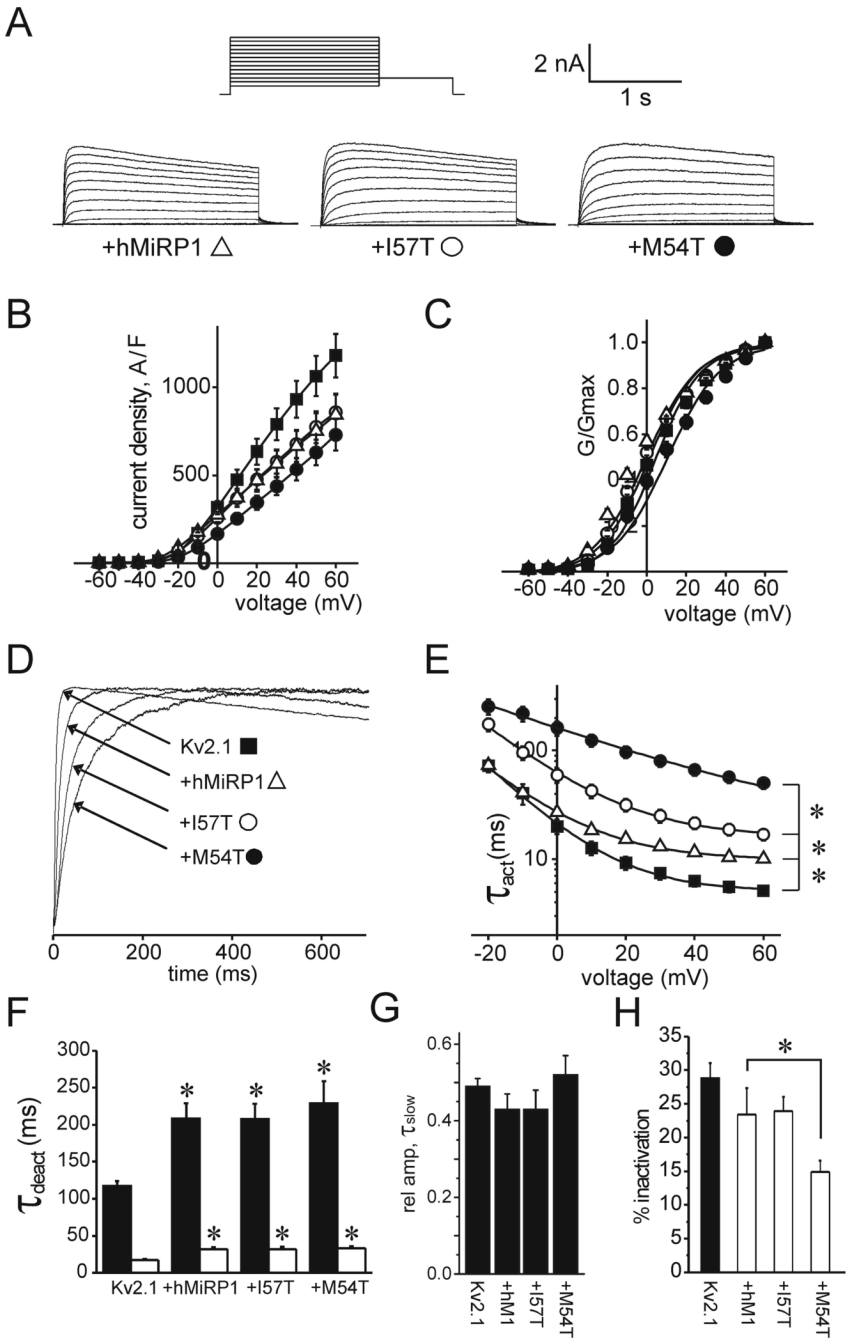

Figure 5. Effects of inherited human MiRP1 mutations on MiRP1-Kv2.1 function

A. Exemplar traces showing currents recorded from CHO cells co-transfected with Kv2.1 + wild-type human MiRP1 ('+MiRP1'), Kv2.1 + I57T-MiRP1 ('+I57T') or Kv2.1 + M54T-MiRP1 ('+M54T'), as indicated. Insets: left, voltage protocol; right, scale bars.

B. Mean peak current density from CHO cells transfected with Kv2.1 alone (filled squares, n = 42) or with wild-type human MiRP1 (open triangles, n = 16), I57T-MiRP1 (open circles, n = 21) or M54T-MiRP1 (filled circles, n = 15).

C. Mean normalized conductance-voltage relationships; cells and symbols as in panel B. Fitting of the data with a Boltzman function, $G = G_{max}/[1 + \exp(V–V_{0.5}/k)]$, gave values for midpoint voltage dependence of activation of: Kv2.1, 4.4 ± 0.7 mV; wild-type hMiRP1-Kv2.1, −0.6 ±

0.8 mV; M54T-MiRP1-Kv2.1, 10.4 ± 1.1 mV; I57T-MiRP1-Kv2.1, 1.1 ± 0.4 mV; slopes were 11.3 ±0.4, 13.1 ± 0.5, 13.4 ± 0.6, and 12.5 ± 0.3 mV, respectively.

D. Normalized exemplar traces showing expanded view of Kv2.1 alone or with wild-type, M54T-or I57T-MiRP1 (as indicated) activation at 0 mV.

E. Mean activation rates at activation voltages between −10 mV and +60 mV, fitted with a single exponential function, expressed as τ_{act}; cells and symbols as in panel B.

F. Mean deactivation rates at −30 mV fitted with a double exponential function, showing slow (black) and fast (white) τ_{deact} components; cells as in panel B, subunits as indicated. * statistically significant difference versus Kv2.1 alone ($p < 0.05$).

G. Mean fractional amplitude of the slow component of deactivation rates of Kv2.1, and Kv2.1 with wild-type or mutant hMiRP1, currents at −40mV fitted with a double exponential function.

H. % inactivation at +40 mV over the initial 1 sec time period; cells as in panel B, subunits as indicated. * statistically significant difference versus wild-type hMiRP1-Kv2.1 ($p < 0.05$).